# Phase separation of crystal surfaces: A lattice gas approach

Joel D. Shore* and Dirk Jan Bukman†
*Department of Physics, Simon Fraser University, Burnaby, British Columbia, Canada V5A 1S6*
(Received 30 August 1994)

We consider both equilibrium and kinetic aspects of the phase separation ("thermal faceting") of thermodynamically unstable crystal surfaces into a hill-valley structure. The model we study is an Ising lattice gas for a simple cubic crystal with nearest-neighbor attractive interactions and weak next-nearest-neighbor repulsive interactions. It is likely applicable to alkali halides with the sodium chloride structure. Emphasis is placed on the fact that the equilibrium crystal shape can be interpreted as a phase diagram and that the details of its structure tell us into which surface orientations an unstable surface will decompose. We find that, depending on the temperature and growth conditions, a number of interesting behaviors are expected. For a crystal in equilibrium with its vapor, these include a low temperature regime with logarithmically slow separation into three symmetrically equivalent facets and a higher temperature regime where separation proceeds as a power law in time into an entire one-parameter family of surface orientations. For a crystal slightly out of equilibrium with its vapor (slow crystal growth or etching), power-law growth should be the rule at late enough times. However, in the low temperature regime, the rate of separation rapidly decreases as the chemical potential difference between crystal and vapor phases goes to zero.

PACS number(s): 64.60.Cn, 68.35.Rh, 68.35.Bs, 64.60.Ht

## I. INTRODUCTION

The decomposition (or "faceting") of a surface into pieces of surfaces of other orientations is a problem of long-standing interest in the materials science and physics communities. It can occur in a variety of circumstances, including when a crystal is being grown or etched [1], when deposition is occurring through such processes as molecular beam epitaxy [2,3], when other materials are adsorbed onto the surface [4], or when an electric current is applied across the sample [5,6]. However, such external perturbations are not always necessary to cause this decomposition: If the surface tension is sufficiently anisotropic, some surface orientations will be thermodynamically unstable [7]. Then, a surface that is initially prepared in such an orientation will spontaneously decompose into a faceted structure, evolving towards a final equilibrium configuration consisting of large facets of stable orientations. This decomposition has been variously referred to as "equilibrium faceting," "thermal faceting," "thermal etching," "Herring reconstruction," or "hill-valley reconstruction" [1,7–9].

Recently, there has been a resurgence of interest in this process in both the experimental [10–12] and the theoretical physics communities [13–16]. In the theoretical community, the close analogy to phase separation of binary liquids or alloys has been pursued. Hence the process has been dubbed "phase separation" or "spinodal decomposition" of crystal surfaces [14,15]. (The terms "faceting," "phase separation," "decomposition," and "coarsening" each have their drawbacks in describing this process in all its various manifestations but, lacking better terminology, we will use all these terms and use them more or less interchangeably.)

The process, which is illustrated in Fig. 1, proceeds as follows. The surface, initially prepared in an unstable orientation, first decomposes into small pieces ("facets") of stable surface orientations, in spite of the fact that this increases the total surface area. The faceted surface then coarsens over time in order to minimize the energy associated with the edges between the different surface orientations. The dynamical process by which the size of the facets grows over time is indeed closely analogous to the phase separation of a binary liquid or alloy, and recent theoretical work has attempted to elucidate the analogy and to investigate the dynamics associated with such separation [13–16]. Much earlier work along these lines was performed by Mullins [9] and he predicted power-law growth of the facet size $L$ with time $t$: $L(t) \sim t^n$ with $n = 1/4$, $1/3$, or $1/2$ for the mass-transfer mechanisms of surface diffusion, volume diffusion, or evaporation condensation, respectively. However, the experimental situation has remained murky. Generally, it has been found that such faceting occurs only very slowly (e.g., $n \approx 0.1$) if at all under near-equilibrium conditions (see the discussion in [16]) and indeed some have argued that such faceting is not even a thermodynamic phenomenon, but occurs only under driven conditions of crystal growth or etching [1]. Nonetheless, it is known theoretically that such faceting should in principle occur in equilibrium if

*Present address: Centre for the Physics of Materials and Department of Physics, McGill University, 3600 University St., Montréal, Québec, Canada H3A 2T8. Electronic address: shore@physics.mcgill.ca

†Present address: Department of Chemistry, Baker Laboratory, Cornell University, Ithaca, NY 14853-1301. Electronic address: bukman@wisteria.tn.cornell.edu

 ©1995 The American Physical Society

the surface tension is sufficiently anisotropic and some of the experimental observations do support this [8,17]. Thus we are led to conclude that one should seek a dynamical explanation to understand why so little faceting is seen [18].

Two of the recent studies of the dynamics have used solid-on-solid approximations of an Ising lattice gas on a cubic lattice with interactions appropriate for alkali halide materials such as sodium chloride (NaCl) [19,20]. Shore, Holzer, and Sethna [13] considered the special case of a [111] surface and argued that the coarsening of the surface should be only logarithmic with time (at long times) for quenches to all temperatures $T$ at which the [111] surface is unstable. This claim was supported by their Monte Carlo simulations. Vlachos, Schmidt, and Aris [16] performed Monte Carlo simulations for the coarsening of $[hk0]$ surfaces, concentrating in particular on a [210] surface. Although they draw no firm conclusions about the asymptotic growth laws, we believe that the results presented there—of anomalously low exponents that decrease with decreasing temperature—are compatible with (although certainly not proof of) logarithmic growth at long times [13,21].

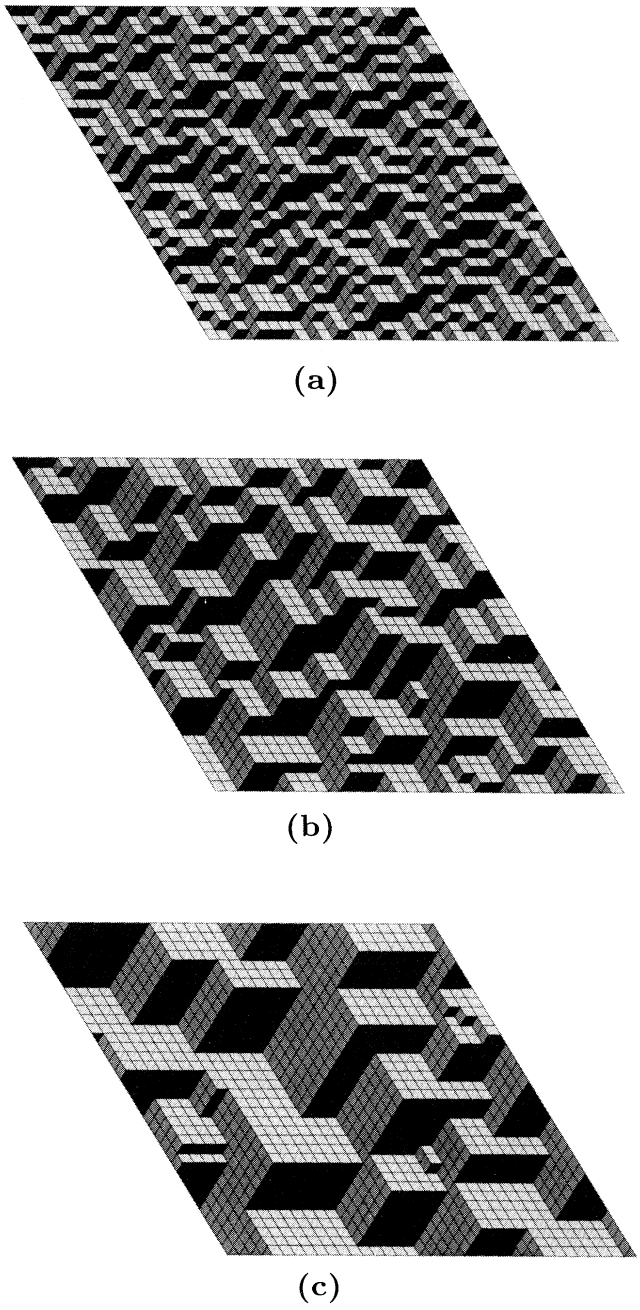


FIG. 1. Decomposition of a surface in the [111] RSOS model for the Hamiltonian of Eq. (1) at $T < T_{CR}$. Shown is a [111] surface that has been quenched from infinite temperature to $T = 3J_2$ at times (a) $t = 0$, (b) $t = 100$, and (c) $t = 10\,000$ (in MC steps per plaquette) following the quench.

The approach of Stewart and Goldenfeld [14] and Liu and Metiu [15] has been along somewhat different lines, closer in spirit to the original work of Mullins. They have looked at the problem in the continuum limit, which is generally claimed to be valid when one is interested in behavior at long times and on long length scales. In this limit, the driving force for the initial breakup of the surface into facets is provided by a sufficiently anisotropic surface tension. Also included in the free energy functional is a term that suppresses rapid changes in the surface normal [15]. Such a term has two effects. First it rounds off the edges and corners on the surface, thus preventing the occurrence of singularities, which would lead to divergences in the Langevin equations. Second, it reproduces, in a macroscopic sense, the energy costs associated with edges and corners, thus providing the driving force for the coarsening of the surface structure. For this model, Liu and Metiu concluded that coarsening proceeds logarithmically for quasi-one-dimensional ordering. Simulations of the resulting Langevin equation for a two-dimensional surface gave $L(t) \sim t^n$ with $n \approx 0.13$ and 0.23 for surface diffusion and for evaporation-condensation mechanisms, respectively. These results were noted to be in fairly good agreement with simple power-counting arguments on the Langevin equation, which suggest $n = 1/6$ and $1/4$ for the two different mechanisms.

Although continuum approaches are a powerful tool and currently enjoy great favor in the study of kinetics of growth, they suffer from at least two major limitations that make it useful to also consider microscopic (e.g., lattice gas) models. The first is that, since they deal with the system on a coarse-grained level, one generally needs to assume some form for the input parameters, in this case the orientation dependence of the surface tension. Thus microscopic models are useful to give us guidance on what form to choose for the surface tension. Indeed, in Sec. III B we will find that the form of the surface tension that arises in one such microscopic model, and may occur quite generally, is considerably different from that which one might have expected from naive considerations.

The second limitation is that such models, at least as currently formulated, appear to be unable to properly model aspects of the problem where the atomic discreteness is fundamental and cannot be ignored. This leads to the conflicting predictions discussed above (logarithmic

vs power-law growth) between the microscopic and the continuum approaches for the coarsening of an unstable [111] surface of NaCl.

The lattice gas models, of course, have their own limitations (e.g., the neglect of elastic effects [18]), but at this point a fairly complete picture of the equilibrium and kinetic aspects of the faceting process within a microscopic model would be useful in advancing the understanding of the faceting process in the real world. In this paper, we will try to present such a unified picture of faceting within the context of the Ising lattice gas model for NaCl. The picture combines and generalizes some of our earlier work on the faceting of a [111] surface [13] and some more recent results concerning the phase diagram of the six-vertex model [22]. We also include a discussion of how the kinetics of the faceting process will be altered for the case of a driven interface, that is, one in which the crystal is being slowly grown or etched.

The outline of the paper is as follows. In Sec. II we introduce the Ising lattice gas model that we will study, discuss the general features of its equilibrium crystal shape (ECS), and explain how the ECS tells us which surface orientations are unstable and into what surfaces such an unstable orientation will decompose. In Sec. III we consider in detail the equilibrium and the kinetic aspects of the phase separation in two different temperature regimes. In Sec. IV we discuss how the kinetics is altered in the case when the crystal is no longer in equilibrium with its vapor (growth or etching). Finally, in Sec. V we present a summary of our conclusions.

## II. EQUILIBRIUM CRYSTAL SHAPE

The problem of determining the equilibrium shape of a crystal by minimizing its total surface free energy subject to a constraint of fixed volume has been considered for over a century [23]. The major result is the celebrated Wulff construction by which one determines the ECS given the surface free energy (surface tension) as a function of the surface orientation.

Only much more recently, however, has the ECS of some simple microscopic models for crystals been considered [19,24–27]. Of particular interest to us is the Ising lattice gas on a simple cubic lattice with nearest-neighbor attractive interactions and next-nearest-neighbor repulsive interactions, first studied by Rottman and Wortis [19]. The Hamiltonian is

$$\mathcal{H} = -J_1 \sum_{\mathrm{NN}} s_i s_j + J_2 \sum_{\mathrm{NNN}} s_i s_j + \frac{\Delta\mu}{2} \sum_i s_i \ , \qquad (1)$$

where the $s_i$ take on the values $+1$ and $-1$. In the lattice gas context, $+1$ is taken to represent an atom occupying the site and $-1$ is taken to represent an empty site. The first sum is over all pairs of nearest neighbors (NNs) while the second is over all pairs of next nearest neighbors (NNNs). We have chosen our sign convention so that both $J_1$ and $J_2$ are positive when the NN bonds are attractive and the NNN bonds are repulsive. We are interested in the case where $J_1/J_2 > 4$, in which case the ground state is (using spin language) "ferromagnetic" [13].

In many instances, it will be useful to consider an interface between occupied and unoccupied sites (i.e., between solid and gas) in the [111] restricted-solid-on-solid (RSOS) approximation [28]. This approximation can be obtained by viewing the interface from the [111] direction and requiring that none of the interface be hidden from view by other parts of the interface (see Fig. 1). It is equivalent to taking the limit $J_1/J_2 \to \infty$ with $T/J_2$ fixed. Configurations in this model can also be viewed as tilings of the plane by 60° rhombi of three different orientations. In this representation, the energetics are reproduced by assigning an energy of $2J_2$ to each border between unlike rhombi and the coarsening process involves the phase separation of the three types of rhombi.

Finally, $\Delta\mu \equiv \mu_s - \mu_v$ represents a difference in chemical potential between solid and vapor. (In spin language it would be a magnetic field.) For the remainder of this paper, with the exception of Sec. IV, we will be considering the case in which the solid and the vapor are in equilibrium ($\Delta\mu = 0$).

The model of Eq. (1) and its RSOS approximation were proposed [20,24] to represent materials such as sodium chloride (NaCl), where the ions of different species (and opposite charge) would have an attractive interaction while those of the same species would repel one another [29]. The ECS for this model is show in Fig. 2. It was found [19] that the ECS remains strictly cubical, with (macroscopically) sharp edges and corners up to the corner-rounding transition at a temperature $T = T_{\mathrm{CR}}$, at which point the crystal first rounds at the corners. For the RSOS model, $T_{\mathrm{CR}}$ can be calculated exactly [20,13] and is given by [30]

$$T_{\mathrm{CR}} = \frac{-4J_2}{\ln[1/3 - 5/(9\alpha^{1/3}) + \alpha^{1/3}]} \approx 7.1124\ldots J_2 \ , \qquad (2)$$

where $\alpha \equiv \frac{1}{6}(\frac{11}{9} + \sqrt{23/3})$. As the temperature is further increased, the rounded region spreads out along the edges until the edge-rounding temperature $T_{\mathrm{ER}}$, at which point the entire edge becomes rounded. The smooth {100}

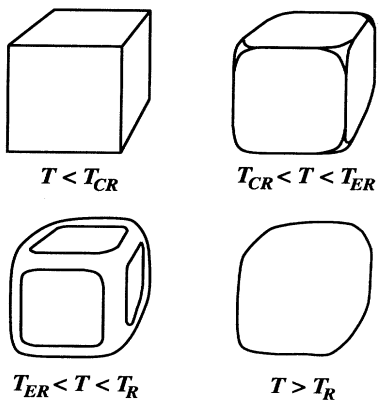


FIG. 2. Qualitative thermal evolution of the equilibrium crystal shape (ECS) for the model specified by the Hamiltonian of Eq. (1), after Ref. [19].

facets still remain, however, up to the roughening temperature $T_R$ [31]. Finally, above $T_R$, the entire crystal shape is rounded.

We make two further observations about these interfacial phase transitions. The first is that when $J_2 = 0$ or is attractive, then $T_{\rm CR} = T_{\rm ER} = 0$. Therefore the corner- and edge-rounding transitions are the result of the competing attractive and repulsive interactions. The second is that within the [111] RSOS model, $T_{\rm ER}$ and $T_R$ are infinite. This is a result of the fact that setting $J_1 \to \infty$ suppresses the fluctuations that are responsible for edge rounding and the roughening of the facets. Thus the usefulness of the RSOS approximation is restricted to temperatures $T < T_{\rm ER}$. It is most reliable for surface orientations close to [111].

Experimentally, in NaCl, the corner-rounding transition is found to occur at a temperature $T_{\rm CR} \approx 920$ K [17,20,24,32]. The sharp cubical shape and the shape with facets but no sharp corners or edges have both been observed experimentally [17]. The intermediate shape with sharp edges but rounding at the corners was also seen on some crystals. However, it is likely that these crystals were not sufficiently equilibrated, so one would have to say that there is, as of yet, no experimental confirmation of this intermediate shape and thus of the claim that the corner- and edge-rounding temperatures are distinct (see [17] and the discussion in [24]).

It is a theorem due to Herring [7] that those surface orientations that do not appear on the ECS are thermodynamically unstable (and will thus break up into pieces of surface of stable orientations). If we represent each surface orientation by a unit vector normal to that surface, then we can use a unit sphere to represent the various surface orientations. For the model specified by Eq. (1), Fig. 3 shows an eighth of such a unit sphere, with shading

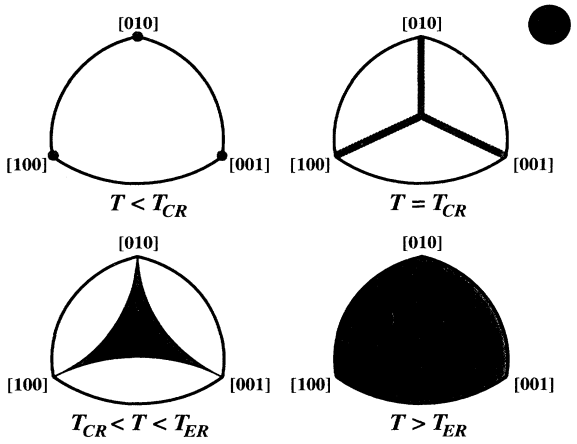


FIG. 3. Stable surface orientations for the model specified by the Hamiltonian of Eq. (1) in various temperature regimes. This figure shows an eighth of a sphere, representing surface orientations by the unit vector normal to the surface. The shaded regions on the figure show those surface orientations that appear on the ECS of Fig. 2. All surface orientations in the unshaded regions are thermodynamically unstable [7] and surfaces prepared in such orientations will decompose into some combination of stable surfaces.

on the sphere used to indicate those surface orientations that are stable in various temperature regimes. Since only the {100} facet orientations appear on the crystal shape (Fig. 2) for $T < T_{\rm CR}$, they are the only stable surface orientations in this temperature regime. At $T_{\rm CR}$, the [111] surface orientation (which is at the center of our diagrams in Fig. 3) and all those orientations on the lines connecting it to the three nearest facet orientations become (marginally) stable. As the temperature is raised further, more and more surface orientations become stable. However, it is not until the temperature reaches $T_{\rm ER}$ that all surface orientations appear on the ECS and are thus stable.

Herring's theorem is actually a specific consequence of a more general fact: The ECS is essentially a phase diagram for the surface orientations [33,24,22]. More precisely, the height of the ECS above a reference plane $F(h,v)$, as a function of the two in-plane coordinates $(h,v)$, can also be considered as a free energy as a function of two "fields" $(h,v)$ [34], which couple to the surface orientation. [$F(h,v)$ is related to the free energy as a function of surface orientation (the surface tension) by a Legendre transformation [33]. Note that here both $F(h,v)$ and the surface tension have been "projected" in the sense that they are free energies per unit area *of the aforementioned reference plane.*]

Because of this mapping between the ECS and a free energy surface, we can transfer all our terminology and knowledge about phase diagrams over to the realm of equilibrium crystal shapes! For example, sharp edges in the ECS are places where $F(h,v)$ has a discontinuity in the first derivatives, i.e., first-order phase transitions, whereas boundaries where a facet smoothly joins the rough regions of the crystal are places where the first derivatives of $F(h,v)$ are continuous but higher-order derivatives are not, and they are thus considered second-order transitions. Even the scaling behavior at these boundaries can be analyzed using the tools of critical phenomena [26,35].

At first-order lines ("edges"), one has coexistence between the two "phases" (surface orientations). The corners of the ECS for $T < T_{\rm CR}$ are points of coexistence between three orientations. Such an interpretation of edges and corners as coexistence lines and points is important because it means that once we know the details of the ECS, we can immediately determine into which surface orientations an unstable surface will decompose. The consequences of this will be further spelled out in the next section where we consider the phase separation process in detail in the two different temperature regimes $T < T_{\rm CR}$ and $T_{\rm CR} < T < T_{\rm ER}$.

## III. PHASE SEPARATION FOR THE CASE OF SOLID-VAPOR EQUILIBRIUM

We first look at a few snapshots of equilibrium configurations of a surface of orientation [15,5,1] in the [111] RSOS model. In Fig. 4(a), we see that for $T < T_{\rm CR}$ the configuration consists of a surface that (apart from a few thermal fluctuations) is phase separated into [100],

[010], and [001] facets. In Fig. 4(b), at a temperature $T_{CR} < T < T_{PS}([15,5,1])$, where $T_{PS}([15,5,1])$ is the phase-separation temperature for this surface, it appears to have separated into one phase vicinal to the [100] facet and another vicinal to the [010] facet. Finally, at a temperature $T > T_{PS}([15,5,1])$, the surface is stable and does not phase separate. These qualitative observations set the stage for our detailed study of the equilibrium and dynamic aspects of the phase-separation problem in the two regimes $T < T_{CR}$ and $T_{CR} < T < T_{PS}([hkl]) \leq T_{ER}$ in which phase separation occurs for an arbitrary surface $[hkl]$.

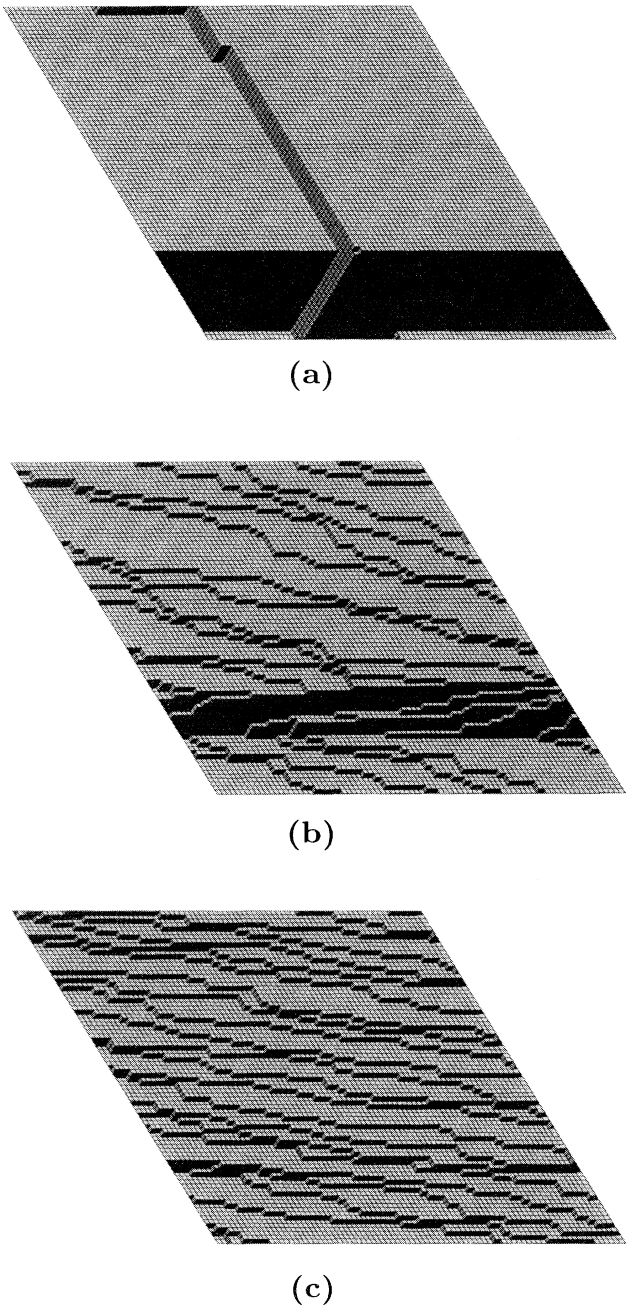


FIG. 4. Equilibrium configurations for a [15,5,1] surface in the [111] RSOS model at various temperatures: (a) $T = 4J_2$, (b) $T = 14J_2$, and (c) $T = 34J_2$. Minimization of the total surface free energy, under the assumption that the surface is close enough to being vicinal that the steps do not interact, gives $T_{PS}([15,5,1]) \approx 22.6J_2$ for the phase separation temperature (see the Appendix and Fig. 7). This estimate should provide an upper bound for the actual value of $T_{PS}([15,5,1])$.

### A. Below $T_{CR}$

In the regime $T < T_{CR}$, all surfaces except the {100} facets are unstable. Any surface prepared in another orientation will decompose into a combination of these surfaces. We can determine which surfaces by utilizing the mapping of the ECS onto a phase diagram discussed above. For example, an arbitrary surface $[hkl]$ with $h$, $k$, and $l$ all positive is a surface that "lives" in the three-phase coexistence region represented by the corner of the ECS where the [100], the [010], and the [001] facets meet. Therefore, such a surface will decompose into a linear combination of these three surface orientations, with the amount of each orientation determined by the requirement that the resulting surface still has the average orientation $[hkl]$. (Electron micrographs of the faceting of the [111] surface of NaCl can be found in Ref. [8], but see also the comments in Ref. [17].) For the special case of a [hk0] surface, the surface lives in the two-phase coexistence region represented by the entire edge between the [100] and [010] facets and therefore decomposition occurs into just these two surface orientations.

In Ref. [13], we gave arguments for logarithmically slow growth of the facet sizes below $T_{CR}$ for the case of the decomposition of a [111] surface. There we also presented strong numerical evidence from Monte Carlo simulations supporting this claim. Although the discussion there was for evaporation-condensation dynamics and within the [111] RSOS model, the same arguments should hold outside the RSOS approximation and should also apply for the case when the dominant mechanism is surface diffusion (in which case the RSOS model is too restrictive to be used). The arguments also generalize to the case of decomposition of any arbitrary surface $[hkl]$.

While the reader is referred to Ref. [13] for the numerical evidence supporting our claim, the basic argument itself is repeated here for completeness: Consider a coarsening surface such as that shown in Fig. 1. At a time $t$, the characteristic length scale (i.e., average facet size) is $L(t)$. In order for the structure to coarsen further, a step across must propagate across one of the facets, for definiteness, say a [100] facet. Since the step consists, microscopically, of pieces of [010] and [001] surface orientations embedded in the [100] surface orientation, the step consists (again, on the microscopic level) of edges between facets of different orientation and thus it costs an energy per unit length. Once the effects of entropy are considered, we find that there is still a nonzero step free energy (i.e., a free energy per unit length) up to $T = T_{CR}$. In fact, within the RSOS approximation, this step free energy as a function of angle can be calculated exactly (see the Appendix). It is only at $T_{CR}$ that this

step free energy goes to zero for a step of a certain angle (specifically, a 45° step).

The coarse-grained differential equation for the growth of $L(t)$ during the coarsening process can be written as [13]

$$\frac{dL}{dt} = \frac{a(L,T)}{L^m} \ . \tag{3}$$

Here $m$ depends on the specific type of dynamics to be considered. For example, for evaporation-condensation dynamics, we likely have $m = 2$ or 3 (see Sec. III B). However, the result below for the asymptotic growth law is independent of $m$.

In the standard case where the kinetic coefficient $a(L,T)$ has no (or only very weak) dependence on $L$, Eq. (3) gives $L(t) \sim t^{1/(m+1)}$. However, here, the fact that the coarsening involves activation over energy barriers of height $f_B(T)L$ implies that the kinetic coefficient $a(L,T)$ decreases exponentially with $L$:

$$a(L,T) = a_0 e^{-f_B(T)L/T} \ . \tag{4}$$

$f_B(T)$ is a free energy barrier per unit length and is related to the step free energy as discussed at the end of the Appendix. At asymptotically long times, Eqs. (3) and (4) imply

$$L(t) \sim \frac{T}{f_B(T)} \ln(t) \ . \tag{5}$$

It is worthwhile to consider this result in the context of the recent work by other groups on this problem. Monte Carlo simulations of the coarsening process for $[hk0]$ surfaces, using essentially the same model as we have discussed above, have recently been presented by Vlachos, Schmidt, and Aris [16]. They consider both the case of the crystal in equilibrium with the vapor and the case where there is a chemical potential difference between them. For the equilibrium case, they found generally slow coarsening with an effective exponent $n_{\rm eff}$ in $L(t) \sim t^{n_{\rm eff}}$, which is small and decreases with decreasing temperature. This scenario is consistent with the behavior found in previous studies of models believed to coarsen logarithmically [13,21]. Since small exponents are hard to distinguish from a logarithm (and the logarithmic form is expected only asymptotically), the ability of Vlachos *et al.* to fit their numerical data to power-law growth with a small exponent should not surprise us.

We should note that the claim by Vlachos *et al.* that a logarithmic form is inconsistent with their data [16] is intended to mean only that a logarithm cannot be fit over the entire time regime [36]. In fact, from the inset of their Fig. 2(b), we see that a logarithm fits quite well (at least as well as a small power law) over the later time regime ($t > 10^2$). The data for shorter times are in the so-called "facet nucleation regime" [16] and can be fitted by neither a logarithm nor a power law. This regime can be understood as the characteristic activation time for depositing or desorbing particles on the initial surface, since the smallest energy barrier of $4J_1$ implies a characteristic time on the order of $t \sim \exp(4J_1/T) \sim 55$ to successfully deposit the first layer on the surface. (Here we use the fact that the energy scale $w_1$ in Ref. [16] is related to ours by $w_1 = 4J_1$.)

Other results presented by Vlachos *et al.,* such as the speeding up of the growth rate when a chemical potential difference exists between crystal and vapor, are at least in qualitative agreement with our picture (see Sec. IV). Thus we can say that the simulations performed in Ref. [16], while certainly not providing very conclusive support for our claims, are at least consistent with them.

The continuum approach of Liu and Metiu [15], by contrast, clearly predicts power-law growth of the facet sizes. How are we to reconcile this difference? Our assertion is that this continuum approach misses a fundamental part of the problem that proves vital to the dynamics in the discrete models (and, we believe, although we are somewhat less certain, in the experimental systems). In particular, in those cases where an unstable surface decomposes into surfaces that are smooth (i.e., below their roughening transition), the dynamics of the faceting of surfaces generically involves the propagation of a step across the facet. Since such a step has a nonzero free energy per unit length for $T < T_{\rm CR}$, this leads to length-scale-dependent barriers and logarithmically slow growth.

Such a dependence is not captured by a continuum model, which does not recognize that there is a smallest size, i.e., the width of a step, determined by the discreteness of the system. Rather, in Ref. [15] the authors introduce a term into their free energy that imposes an energy cost for rapid changes in surface orientation. This captures some of the physics that arises in the microscopic models, but clearly not all of it. Furthermore, because the Langevin equations cannot cope with singularities (and in keeping with the spirit of coarse graining), they round the cusps in the surface tension associated with the crystal facets. This means, in effect, that there is no longer any roughening transition in the model: all surface orientations are rough.

The idea that the discreteness of a crystal is fundamental in determining dynamical, and even equilibrium, behavior is certainly not without precedent. The very existence of a roughening transition and of nucleated dynamics for crystal growth below this transition is dependent upon including terms in the Hamiltonian (and the resulting dynamical equations) that explicitly model the discreteness of the system [37–40]. As far as we know, there is no known prescription for determining *a priori* whether such discreteness will be relevant or irrelevant in a renormalization group sense. In the absence of such a prescription, purely continuum approaches to the problem (even if they mimic some effects produced by the discreteness, e.g., by using anisotropic surface tensions and energy penalties for changes in surface orientation) should, we believe, be used with a certain degree of caution.

In Sec. IV we will return to the case of coarsening below $T_{\rm CR}$, but in the case where the crystal is slightly out of equilibrium with the vapor. There we will find that the difference in chemical potential between vapor and crystal sets a maximum size to the free energy barrier, so the problem becomes one of nucleation and there is a return to power-law behavior at late enough times. How-

ever, first we will consider the coarsening process for the case of crystal-vapor equilibrium but in the temperature regime above $T_{CR}$.

### B. Above $T_{CR}$

When we consider the diagram in Fig. 3 showing the stable orientations at a temperature $T_{CR} < T < T_{ER}$, three questions immediately present themselves: (1) How does one determine the location of the boundaries between the stable and unstable surface orientations? (2) For a surface in the unstable region, what are the orientations of the stable surfaces it breaks up into? (3) What are the kinetics of this process?

#### *1. Equilibrium aspects*

We find it most natural to begin with a discussion of the second question raised above. The behavior of an unstable surface depends on the details of the ECS. In Figs. 5 and 6, we consider two possible scenarios [41].

In Fig. 5(a), for what we dub the "ridge scenario," the sharp edges ("ridges") between the facets continue into the curved region of the ECS. As one moves along such a ridge into that region, the angle between the unit vectors normal to the two surfaces that meet at that point on the ridge decreases from 90° at the facets to 0° at a second-order point at which the ridge terminates. Since at any point along this ridge two surface orientations meet, the mapping of the ECS onto a phase diagram tells us that this means there is coexistence between two surface orientations at each point. Without loss of generality, we consider the case of a surface $[hkl]$ with $h \geq k \geq l > 0$. Figure 5(b), showing part of the diagram of stable surface orientations, demonstrates how such a surface prepared at an unstable orientation breaks up into two surfaces. Note that, by symmetry, the two coexisting surfaces are symmetric about the line $h = k$. Also, a linear combination of these two surface orientations must add up to give an average surface orientation of $[hkl]$. These two conditions, along with the third condition specifying those surfaces that are on the curve of marginally stable surfaces, completely specify the two surfaces that the surface $[hkl]$ decomposes into.

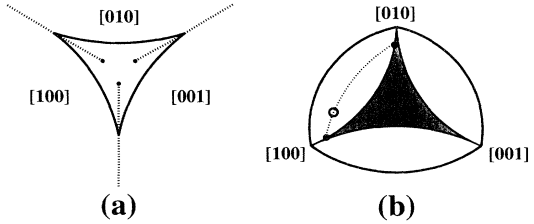


FIG. 5. The "ridge scenario." In (a) we show a closeup of the corner region of the ECS for $T_{CR} < T < T_{ER}$, under the assumption that the sharp edges between the facets continue into the curved part of the ECS, finally terminating at second-order critical points. At any point along this edge, there is "coexistence" between two surface orientations. (Here sharp first-order edges are shown by dashed lines while the second-order Pokrovsky-Talapov boundaries between the facets and the curved part of the ECS are shown by solid lines. The solid circles represent second-order critical points at the end of the first-order lines.) In (b) we present the diagram of the stable surface orientations, showing how any unstable surface will phase separate into the two coexisting stable surfaces. In our example, any orientation along the dashed curve (such as the one indicated by the open circle) decomposes into the two (marginally) stable surface orientations indicated by the solid circles.

In Fig. 6(a), which we dub the "conical point scenario," the sharp edge terminates at the point where it meets the facet boundaries. (This can be considered as a limiting case of taking the length of the ridges into the curved regions to zero.) In this case, all the unstable surfaces must live in the point where the edge meets the facet boundaries. Furthermore, all the marginally stable orientations along the boundary in Fig. 6(b) must meet at this one point on the ECS. The slope of the ECS at this point depends on the angle from which it is entered. Therefore, in the rounded region of the ECS, the point has the symmetry of the tip of a cone, hence the name "conical point." Also note that the ECS has a jump in slope as one goes from the rounded region of the ECS, through the conical point, and onto one of the facets (or, alternately, along the sharp edge between the two facets) [42].

Naively, one might expect that the ridge scenario would occur in general, as the conical point scenario seems to require that there be special symmetry about the conical point, which results in the meeting of all the different orientations at this single point on the ECS [43]. Such a point is very much analogous to the zero field ($\mathbf{H} = \mathbf{0}$) point in the low temperature phase of a three-dimensional $XY$ model, at which an entire one-parameter family (circle) of magnetizations coexist. However, in that model such degeneracy is clearly the

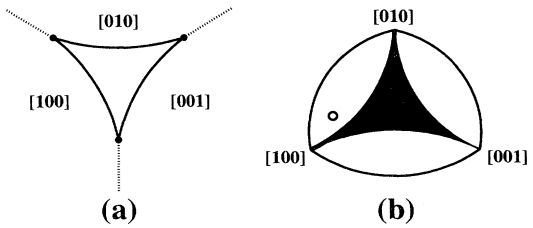


FIG. 6. The "conical point scenario." In (a) we show the corner region of the ECS for $T_{CR} < T < T_{ER}$, under the assumption that the sharp edge between the facets terminates at the point where it meets the curved region of the ECS. At this conical point (indicated by a solid circle), an entire one-parameter family of surface orientations coexist. In the curved part of the crystal shape, these orientations come together at this point just as they do at the tip of a cone. In (b) we present the diagram of the stable surface orientations, showing how an arbitrary unstable surface orientation (shown by an open circle) will decompose into a combination of the entire one-parameter family of coexisting surface orientations (shown by the bold solid curve).

result of the symmetry with respect to spin orientation $\theta$ that occurs for $\mathbf{H} = \mathbf{0}$ in the original Hamiltonian. In the present problem, there is no such obvious symmetry and thus such a point would not be expected unless the terms breaking this symmetry become irrelevant under renormalization of the original Hamiltonian.

To rigorously determine which scenario occurs in one specific model, we have recently studied [22] the [110] RSOS model for the surface of an fcc crystal with nearest-neighbor attractive and next-nearest-neighbor repulsive interactions [26]. In this model, $T_{\rm CR} = 0$, i.e., the corners round for any $T > 0$. However, a sharp edge separating the [111] and the $[11\bar{1}]$ facets persists up to a nonzero temperature $T_{\rm ER}$.

The advantage of this model is that it can be mapped onto the six-vertex model [26,44] that is exactly solved [45,46]. The solution of the six-vertex model, which is given in terms of integral equations, can be investigated numerically and, in certain limits, analytically [22]. We find that in this model, the conical point scenario occurs, as was conjectured by Jayaprakash and Saam [26] at the time when they first considered this RSOS model [47]. Furthermore, we find interesting nonanalytic scaling behavior in the curved region of the ECS as one moves away from the conical point [22]. Note that such nonanalytic scaling behavior at a first-order coexistence boundary cannot be explained within mean field theory, where first-order transitions are associated simply with crossings in the local minima in the free energy surface. It is only through the effects of renormalization that such nonanalytic behavior can appear.

Clearly, the question that must be asked is how generally a conical point occurs, as opposed to having a ridge extend into the rounded region of the ECS. We are not able to answer this question rigorously. However, we believe that the evidence from the six-vertex model suggests that the conical point will be a general feature of equilibrium crystal shapes at the point where a sharp edge between facets meets a rounded region of the ECS. This belief is based upon the following observation: In the six-vertex model, the appearance of the conical point, having such a high degree of symmetry, does not seem to be due to any special symmetry that already exists in the original Hamiltonian. Rather, the symmetry seems to be generated spontaneously under renormalization (and this occurs for *all* temperatures and values of the interaction parameters that put us in the "low temperature ferroelectric regime" of the model). Therefore, we expect such conical points with the associated scaling behavior to be a rather generic feature of equilibrium crystal shapes, probably occurring for simple cubic as well as fcc models and outside the RSOS approximation. On the other hand, Neergaard and den Nijs have recently presented an argument that the conical point, or at least the specific scaling exponents at this point, may be a rather special feature of the six-vertex model [48]. In light of these conflicting opinions, we must say that the generality of this feature remains an open question.

It is interesting to note that the conical point in the crystal shape and the associated coexistence region in the space of surface orientations is precisely the converse of a conical point (cusp) in the surface tension and the associated flat facet on the crystal shape $F(h, v)$ [49]. The analog of the one-parameter family of orientations coexisting for the former case is the one-parameter family of points on the crystal shape (namely, those on the boundary of the facet) that all correspond to the cusp point in the surface tension. Also, the sharp edge, or ridge, between the facets in $F(h, v)$ is analogous to the "groove" in the surface tension that exists between the two coexistence regions associated with the two conical points [22].

We are now ready to discuss the first question posed at the beginning of Sec. III B, namely, the determination of the boundaries between stable and unstable orientations as a function of temperature $T_{\rm CR} < T < T_{\rm ER}$ (see Fig. 3). These boundaries can in fact be determined exactly for the fcc case, within the [110] RSOS approximation, because of the mapping onto the exactly solved six-vertex model [22]. For the simple cubic case, we do not have an exact solution even within the [111] RSOS approximation. However, we can calculate the "opening angle" $\theta_c(T)$ for this curve. [In Fig. 6(b), this is the opening angle between the bold solid line and the octant boundary.] This angle is also half the opening angle $2\theta_c(T)$ between the two facet boundaries on the ECS at the conical point. Because calculation of $\theta_c(T)$ involves surfaces that are vicinal to the facet orientations (i.e., the steps across the facets are widely spaced so that step-step interactions are not important), it can be determined from an exact calculation of the free energy of an isolated step within the [111] RSOS approximation. The calculation of the step free energy $f_s(T, \theta)$ and the angle $\theta_c(T)$ are discussed in the Appendix. An alternate way to view $\theta_c(T)$ is that its inverse function $T_{\rm PS}(\theta)$, gives the "phase-separation temperature" for a vicinal surface (i.e., that temperature below which the surface is unstable) as a function of the angle of the steps across the surface (and thus its orientation). A plot of $T_{\rm PS}(\theta)$ is given in Fig. 7.

We have carried out some simulations of the breakup of various surfaces $[hkl]$ with $h \geq k \geq l > 0$ at various temperatures. Those surfaces studied that are in the limit $l \ll h$ ($[15, 5, 1]$, $[22, 7, 1]$, and $[30, 29, 1]$ surfaces) appear to decompose into two phases, one vicinal to the [100] surface and the other vicinal to the [010] surface [see, e.g., Fig. 4(b)]. When the system is quenched from high temperatures, thin stripes of these two vicinal phases form and then coarsen over time until only one stripe of each phase remains in the system. We have measured the approximate angles of the steps across these vicinal phases and find that they are in quite good agreement with our formula for $\theta_c(T)$ (see Fig. 7).

Note that the surface appearing to decompose into only two surface orientations, rather than an entire one-parameter family, seems to be in contradiction to the conical point scenario that we have argued is likely to apply. However, three important points should be stated. The first is that it is in fact hard to tell if there are really only two orientations present. What we can say with confidence is that there seems to be a breakup into a phase with orientations near [100] and a phase with orientations near [010] and that both these phases consist

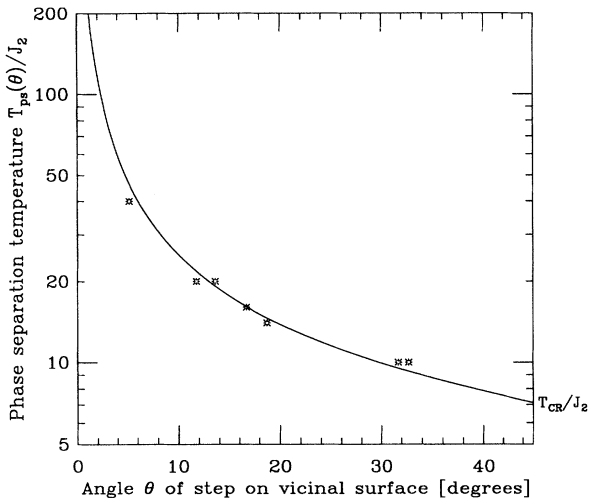


FIG. 7. Phase separation temperature $T_{\rm PS}(\theta)$ for a vicinal surface as a function of the angle of the steps across it in the [111] RSOS model, as calculated in the Appendix. Alternatively, as explained in the text, the inverse function $\theta_c(T)$ can be thought to represent the angle of the steps across the vicinal surfaces that an unstable crystal surface $[hkl]$ with $0 \leq k \leq h$ and $0 \leq l \ll h$ decomposes into. The symbols represent measurements of $\theta_c(T)$ from simulations of this decomposition process. For a finite value of $J_1/J_2$ (i.e., relaxing the RSOS constraint), the curve would look qualitatively similar for large angles but would not diverge as $\theta \to 0$. Instead, we would have $T_{\rm PS}(\theta \to 0) = T_{\rm ER}$.

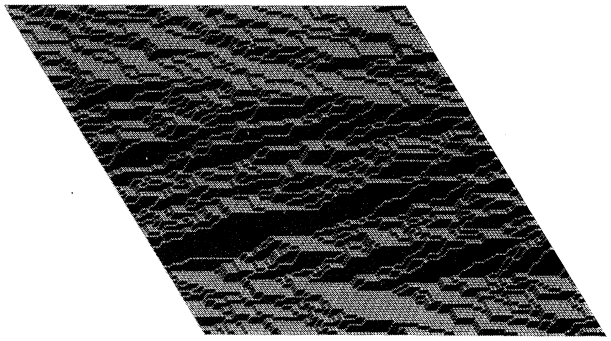

FIG. 8. Equilibrium configuration for a [13,13,4] surface in the [111] RSOS model at $T = 8J_2$. Note that the surface appears to have phase separated, but the equilibrium state is quite complicated. This may be an indication that many different surface orientations are involved, as one would expect from the conical point scenario.

of vicinal surfaces with steps having approximately the angle $\theta_c(T)$ across them. This is not really in contradiction with what we expect: In the conical point scenario, the decomposition will consist of a weighted distribution of the surfaces in the one-parameter family of marginally stable orientations. For decomposition of a surface close to being a $[hk0]$ surface, the decomposition must primarily consist of those surfaces vicinal to the [100] and the [010] surfaces in order to get the correct average surface orientation. (For a $[hk0]$ surface itself, the decomposition will simply be into the [100] and the [010] surface orientations.)

Our second point is that when we then carry out simulations of surfaces that are not as close to being an $[hk0]$ surface (and at temperatures nearer to $T_{\rm CR}$ in order that we see any phase separation at all), then the equilibrium configurations do not appear to be so simple. Figure 8 shows an equilibrium configuration of a $[13, 13, 4]$ surface at $T = 8J_2$. At $T = 9J_2$, the configurations are even more complicated and it is in fact hard to tell if the surface has phase separated at all. Unfortunately, in studying these configurations, we have found it difficult to quantify the surface phase separation since one would have to measure the surface orientation coarse grained over some region, because (unlike, e.g., in the case of an $XY$ model) the order parameter is not a continuous variable at the microscopic level: each rhombic tile represents either a [100], a [010], or a [001] orientation. The correct scale over which to coarse grain is not obvious and, of course, the larger this scale, the larger the system size should be in order to avoid finite-size constraints.

Our final point is that the periodic boundary conditions put some constraints on the system, specifically, that the stripes of each phase in Fig. 4(b) must be horizontal. This may be influencing the results considerably. Therefore, one might need to go to much larger system sizes (which is not computationally feasible at present) in order to start truly seeing the other available surface orientations. Another approach would be to try to choose alternative boundary conditions (such as free or helical). However, implementing such boundary conditions and forming the initial surface configuration is a nontrivial task in this model.

In the final analysis, we would have to say that the simulations currently do not provide conclusive evidence either for or against the conical point scenario in this model.

### 2. *Kinetics*

To study the kinetics of the phase ordering process, we turn to the continuum formalism used by Liu and Metiu [15]. For the case of the evaporation-condensation mechanism, and neglecting noise since temperature is believed to be an irrelevant variable, they derived the Langevin equation

$$\frac{\partial \boldsymbol{\psi}(\mathbf{r},t)}{\partial t} = -A\left[a\nabla^4\boldsymbol{\psi}(\mathbf{r},t) - \nabla\left(\nabla\cdot\frac{\partial F_0(\boldsymbol{\psi})}{\partial \boldsymbol{\psi}}\right)\right], \quad (6)$$

where $\mathbf{r} \equiv (h, v)$ and $\boldsymbol{\psi}$ is a vector specifying the surface orientation. (Here we have used the constraint $\nabla \times \boldsymbol{\psi} = 0$ to rewrite the first term on the right-hand side [3]. This constraint follows from the fact that $\boldsymbol{\psi}$ is the gradient of the surface.) If surface diffusion is the dominant mechanism, then there is an additional $-\nabla^2$ in front on the right-hand side. $F_0(\boldsymbol{\psi})$ is some suitably coarse-grained projected surface tension, not the full thermodynamic projected surface tension. In particular, $F_0(\boldsymbol{\psi})$ is not necessarily convex since, in the case when the $\boldsymbol{\psi}$ orienta-

tion is unstable, it reflects the free energy of metastable configurations having orientation $\psi$ rather than the thermodynamic configurations once phase separation has occurred (see, e.g., Ref. [50]). The term "projected" refers to the fact that the surface tension is a free energy per unit area *of some reference plane*, as discussed in Sec. II.

Because the order parameter $\psi$ is conserved, the stable stationary states (i.e., those orientations into which a surface decomposes) are not simply given by the minima of $F_0(\psi)$. Rather they are given by those values of $\psi$ that share a common support tangent on $F_0(\psi)$ (see, e.g., Fig. 3 in Ref. [15]).

Note that the structure of Eq. (6) is *very* similar to that for the traditional phase separation process, i.e., the so-called Cahn-Hilliard equation (see [51]). The one difference is the reversal of the ordering of the two vector operators in the second term on the right-hand side: Here we have the gradient of a divergence (and also the constraint that $\nabla \times \psi = 0$), while in the traditional case one has the divergence of a gradient [3]. The former case causes a coupling of the different components of the order parameter, and of the spatial and order-parameter degrees of freedom, while the latter case leaves them uncoupled. (In fact, the former case only makes sense if $n = d$, where $d$ is the spatial dimension of the interface and $n$ is the number of degrees of freedom of the order parameter.)

Before considering the case of most interest to us at present (where phase separation is expected to occur into a continuous family of orientations), we will first discuss the "simpler" case of separation into a finite number of orientations. This has been the subject of much very recent work. In Ref. [15], the authors assumed a form for the surface tension that results in a few (e.g., three) stable stationary states in $F_0(\psi)$. On the basis of simulation results and power counting, they argued that the growth of the domain size likely satisfies $L(t) \sim t^{1/4}$. However, in the case of traditional phase separation (i.e., governed by the Cahn-Hilliard equation) into a finite number of phases, such power counting is known to fail. Because of the sharpness of domain walls, one finds instead $L(t) \sim t^{1/3}$. The most general arguments for these results are given by Bray [51], who argues that the growth law in the case of conserved dynamics can be determined from the energy cost of a domain wall. If the energy cost goes like $E(L) \sim L^y$, then $L(t) \sim t^{1/(2+d-y)}$. For the case of sharp domain walls, e.g., in an Ising model, $y = d - 1$, whereas in the case of domain walls that are spread out over a width $L$, as in the isotropic vector spin models, $y = d - 2$.

Do Bray's arguments continue to hold for Eq. (6) or does the reversal in the order of the vector operators result in different behavior? It appears that, in fact, the renormalization flow equations change such that simple connection between $y$ and the growth law exponent no longer necessarily follows [3]. Indeed, in addition to Liu and Metiu [15], a few other groups have recently simulated equations similar to Eq. (6) and have found results most compatible with $L(t) \sim t^{1/4}$ [3,6]. Thus it seems possible that the order of the vector operators does change the kinetics of the phase separation process. On the other hand, given the history of low measured exponents (often around 1/4) in Ising systems where eventually the exponent was shown to cross over to 1/3 [52], we believe that, in the absence of further analytical understanding, both $L(t) \sim t^{1/4}$ and $L(t) \sim t^{1/3}$ (or even some intermediate exponent) should still be considered as viable candidates for the asymptotic behavior.

Finally, we note that we have also published some of our own numerical evidence bearing on this question. In Ref. [13], we looked at the behavior of the characteristic length scale for the coarsening of a [111] surface cooled slowly *at a constant rate* $\Gamma$. Assuming the "underlying growth law" in the absence of diverging barriers would be $L(t) \sim t^{1/3}$, we argued that the behavior under asymptotically slow cooling would be $L(\Gamma, T = 0) \sim \Gamma^{-1/4}$. It was noted that this expectation was in reasonable agreement with our numerical results. Here we add two comments: (1) If the "underlying growth law" is instead $L(t) \sim t^{1/4}$, then the corresponding behavior at a constant cooling rate is $L(\Gamma, T = 0) \sim \Gamma^{-1/5}$ (see endnote 68 of Ref. [13]). (2) The simulations performed there, and further simulations carried out on systems as large as $240^2$ [53], cannot conclusively distinguish these two possibilities, with the best estimate of the exponent of $\Gamma$ being $-0.23$, i.e., about halfway between the two expectations.

Of course, the considerations of the previous three paragraphs apply to the case where the surface tension is such that phase separation occurs into a finite number of different orientations separated by sharp domain walls. This will be relevant to our discussions in Sec. IV. In the present case, however, our $F_0(\psi)$ is expected to be of such a form that we have phase ordering into a continuous one-parameter family of orientations. The numerical work of Siegert and Plischke [3] suggests that in this case, as in the standard case when the vector operators are reversed (e.g., an isotropic $XY$ or Heisenberg model), the exponent for the growth law is 1/4. (Note, however, that, technically speaking, the case $n = d = 2$ is excluded from Bray and Rutenberg's theory of phase ordering in the Cahn-Hilliard equation because of long-range correlations between the topological defects [51]. Simulations of this case are nonetheless consistent with $L(t) \sim t^{1/4}$, but perhaps with logarithmic corrections and deviations from scaling [54].)

It is worth emphasizing that the whole decomposition process here is quite different from the case where separation occurs into a finite number of orientations: Here, there are really no well-defined domains or "facets" formed at all; rather, it is the length scale over which the surface bends that will increase over time (which can be measured most easily from a correlation function or its Fourier transform). Thus terms such as "faceting" and "phase separation" seem somewhat inappropriate.

## IV. CRYSTAL GROWTH OR ETCHING

We now consider the case in which the crystal is slightly out of equilibrium with its vapor, that is, the case of slow growth or etching. In fact, it is known that, far

out of equilibrium, the nonequilibrium effects can drive the formation of facets even when such faceting would not occur in equilibrium [3,6]. Here, however, we will assume that we are close enough to equilibrium that the stability of a surface is still determined from equilibrium considerations and will study the effect of a chemical potential difference $\Delta\mu$ between solid and vapor phases [16] on the dynamics of the phase separation. In the magnetic language of the three-dimensional Ising ferromagnet, such a situation can be thought of as the application of a uniform magnetic field in the model.

First we consider the temperature regime $T < T_{CR}$ and, for definiteness, we discuss the case of crystal growth ($\Delta\mu < 0$). Then the free energy cost associated with adding surface atoms to produce a step across a facet can be written approximately as

$$\Delta F \approx f_p(T,\theta)L - |\Delta\mu|\frac{L^2}{2}\tan(\theta) \ . \tag{7}$$

Here $f_p(T,\theta)$ and $L$ are the projected step free energy and the projected length of the step, respectively (see the Appendix). The projection is onto one of the lattice axes and $\theta$ is the angle of the step relative to that axis. [Equation (7) is valid when the linear size of the facet itself is larger than $L$.] The structure of the problem is the same as that of determining the growth rate (due to nucleation) of a growing crystal surface at a temperature below its roughening transition [38]: Assuming that $|\Delta\mu|$ is not too large, then for small $L$ the first term in the expression dominates and $\Delta F$ increases linearly with $L$. However, for large enough $L$, the second term dominates and $\Delta F$ is a decreasing function of $L$.

To find the smallest possible barrier associated with propagating a step across an infinite facet, we want to find the length of step $L_0$ and the angle $\theta_0$ such that the free energy cost is maximized as a function of $L$ and minimized as a function if $\theta$. This we do by setting $\partial(\Delta F)/\partial L = \partial(\Delta F)/\partial\theta = 0$. We find

$$L_0 \approx \frac{f_p(T,\theta_0)}{|\Delta\mu|\tan(\theta_0)} \ , \tag{8}$$

with an implicit expression for $\theta_0$ given by

$$\left.\frac{\partial f_p(T,\theta)}{\partial[\tan(\theta)]}\right|_{\theta=\theta_0} = \frac{f_p(T,\theta_0)}{2\tan(\theta_0)} \ . \tag{9}$$

However, this latter expression always has the solution $\tan(\theta_0) = 1$, independent of $\Delta\mu$ or $T$, so a step of 45° always gives the smallest barrier. Thus (8) becomes

$$L_0 \approx f_p(T,\theta=\pi/4)/|\Delta\mu| \tag{10}$$

and the free energy barrier is

$$\Delta F_{\max} \approx \frac{f_p^2(T,\theta=\pi/4)}{2|\Delta\mu|} \ . \tag{11}$$

Equation (11) gives the maximum size of the barriers for a coarsening surface. The barriers to coarsening will grow and thus the coarsening of the surface will look roughly logarithmic, out to a time of order

$$t_c \approx \exp[f_p^2(T,\theta=\pi/4)/(2|\Delta\mu|T)] \tag{12}$$

when the characteristic facet size $L$ is of order $L_0$. At times longer than this, the barrier height to coarsening remains saturated at $\Delta F_{\max}$, independent of $L$, and the growth will thus proceed with a power law

$$L(t) \sim (\gamma t)^n \ , \tag{13}$$

with $\gamma \approx \exp[-f_p^2(T,\theta=\pi/4)/(2|\Delta\mu|T)]$. Here $n$ is the exponent for growth associated with Eq. (6) in the case where the surface breaks up into a finite number of orientations (thus either $n = 1/3$ or $n = 1/4$, as discussed in Sec. III B 2).

The form of $\gamma$ is closely analogous to that for the rate of growth of a defect-free crystal surface below the roughening transition [38]. The one important difference, however, is that in this latter case, no driving force exists for the growth of the crystal in the limit $\Delta\mu = 0$. In the case of the phase separation problem, however, while there is still no driving force *for growth of the crystal* in the absence of a chemical potential difference, there *is* a driving force *for phase separation of the surface.* Thus the characteristic length scale grows with time even when $\Delta\mu = 0$, but the process occurs logarithmically slowly in this case.

We have performed Monte Carlo simulations of the [111] RSOS model in order to test certain aspects of our above arguments. First, in order to study the tenet of our argument involving the behavior of the free energy barrier as a function of the size of the facet [Eq. (7)], we consider the process of removing one face of a "cubical projection" from a crystal surface, as illustrated in Fig. 9. Figure 10 is an Arrhenius plot of the time such a process takes as a function of the linear size $L$ of the projection for the case $\Delta\mu = 0$. (Cf. Fig. 6 of [13] where a similar plot was presented for the case of fully three-dimensional coarsening. Also see that reference for further details about the simulation methods.) We see that, as is our expectation, the slope on the Arrhenius plot, and thus the free energy barrier, is an increasing function of the size of the projection. In fact, the expected free energy barrier in the limit $T \to 0$ can easily be calculated [55] to be

$$F_B(L,T=0) = \begin{cases} 12J_2 \ , & L = 2 \\ 4J_2(L+2) \ , & L > 2 \ . \end{cases} \tag{14}$$

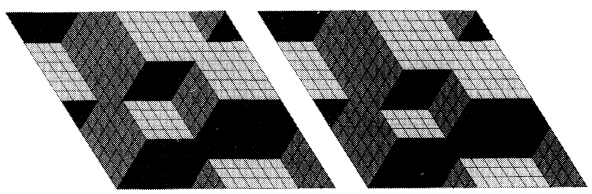

(a) (b)

FIG. 9. Shrinking a cubical projection in the [111] RSOS model. (a) Cubical projection with $L = 4$. (b) Same projection once one face has been removed. For $\Delta\mu \geq 0$, this configuration is lower in energy than that of (a) by $4J_2 + \Delta\mu L^2$.

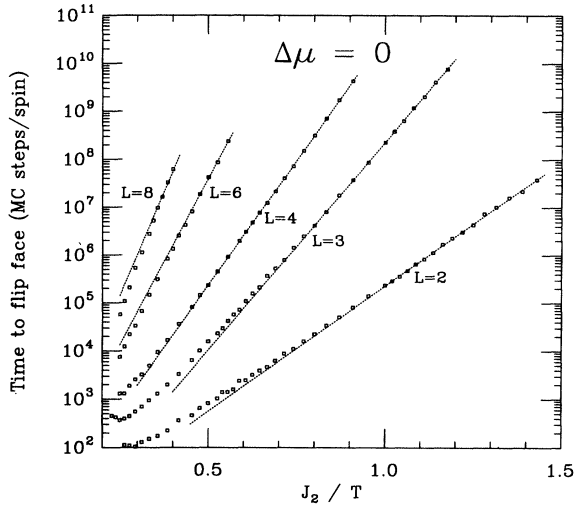


FIG. 10. The time to shrink a cubical projection for $\Delta\mu = 0$. Shown are the results of Monte Carlo simulations for the average time to remove the first face from a cubical projection of size $L$ [such as that shown in Fig. 9(a)] for the case $\Delta\mu = 0$. Each point is an average over 900 runs with standard error smaller than the symbol size. The dotted lines are one-parameter fits to the form $t = t_0(L)e^{F_B(L,T=0)/T}$ with $F_B(L,T=0)$ given by Eq. (14) and $t_0(L)$ a free parameter. Between 4 and 15 of the lowest temperature data points are used for each fit.

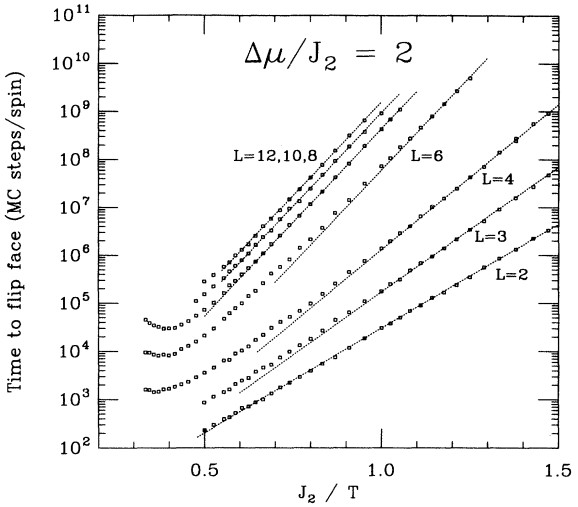


FIG. 11. The time to shrink a cubical projection for nonzero $\Delta\mu$. Shown are the results of Monte Carlo simulations for the average time to remove the first face from a cubical projection of size $L$ for the case $\Delta\mu/J_2 = 2$. Each point is an average over 900 runs with standard error smaller than the symbol size. The dotted lines are one-parameter fits to the form $t = t_0 e^{F_B(L,T=0)/T}$ with $F_B(L,T=0)$ given by Eq. (15) and $t_0(L)$ a free parameter. Between 6 and 18 of the lowest temperature data points are used for each fit. For $L \leq 4$, some of the fitted data lie off scale.

Fits to the form $t = t_0(L)e^{F_B(L,T=0)/T}$, with $t_0(L)$ as a free parameter, are also shown in the figure and are generally very good for the low temperature data. Only for $L = 8$ are systematic deviations from the fits still evident at the lowest temperatures, with the slope on the plot being *greater* than that predicted. This deviation is due to our approximation of $F_B(L,T)$ by $F_B(L,T=0)$ (see Sec. II of Ref. [13]).

In Fig. 11 we present an Arrhenius plot for the time to shrink a cubical projection of size $L$ for $\Delta\mu/J_2 = 2$. (Here the sign of $\Delta\mu$ is chosen to be positive, i.e., to favor shrinking of the projection.) The contrast to Fig. 10 is apparent: For small $L$, the free energy barrier is an increasing function of $L$. However, for $L \geq 6$, the barrier appears to saturate. The expected barrier for each $L$ can in fact be calculated by considering the highest energy state the system must pass through in removing a face on the projection. This gives

$$F_B(L,T=0) = \begin{cases} 12J_2 - \Delta\mu\ , & L = 2 \\ 4J_2(L+2) - \Delta\mu(L+1)\ , & 2 < L \leq 6 \\ 18J_2\ , & L \geq 6\ . \end{cases} \tag{15}$$

(Here the saturation of the barrier at $L = 6$ is for the specific case of $\Delta\mu/J_2 = 2$.) Fits to the form $t = t_0(L)e^{F_B(L,T=0)/T}$, with $t_0(L)$ as a free parameter, are also shown in the figure and are generally very good for the low temperature data. (The one fit that shows a bit of deviation is for $L = 6$, probably because of the presence of a large degeneracy of barrier states with very similar barrier heights.) Also, the value of $18J_2$ that we get for the saturated barrier height is in quite good agreement with the estimate of $16J_2$ provided by Eq. (11) in the limit $T \to 0$ [which can be worked out using Eq. (9) and formulas in the Appendix].

The preceding study tested our assertions about the barrier heights to coarsening for one very artificial kind of configuration. In order to test more directly the effect of a nonzero $\Delta\mu$ on the coarsening process, we present in Fig. 12 full-scale simulations of the coarsening of a [111] surface, which is initially in a random ($T = \infty$) configuration and is quenched to $T = 2J_2$. The figure shows the growth of the characteristic length scale $L(t)$ over time for various values of $|\Delta\mu|/J_2$. We see that, in its qualitative aspects, the Monte Carlo data are in agreement with our expectations. First, we consider the case $\Delta\mu = 0$. The growth, although not yet quite logarithmic as would be expected at asymptotically long times, is slower than a power law; the effective exponent in $L(t) \sim t^{n_{\rm eff}}$ is $n_{\rm eff} \approx 0.07$ at the latest times and is continuing to slowly decrease.

As the chemical potential difference between solid and vapor is increased from zero, the growth becomes faster. For $|\Delta\mu|/J_2 = 0.5$, the effective exponent is virtually constant over the six decades of time shown. For the larger $|\Delta\mu|$, the increase in the effective exponent with time is quite gradual. However, the most marked bending of the data does appear to occur at times whose trend with $|\Delta\mu|$ is in qualitative agreement with (but that seem to be quantitatively a bit later than) the expectations of Eq.

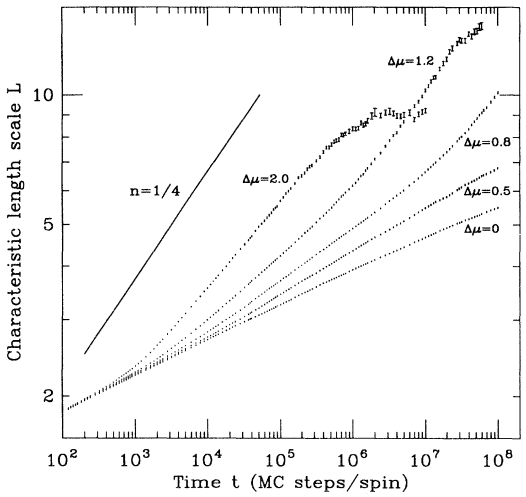


FIG. 12. Growth of the characteristic length scale $L(t)$ during coarsening of a [111] surface at $T = 2J_2$ for various values of $\Delta\mu$ (given on the figure in units of $J_2$). The runs were performed on a $120^2$ system. For each value of $\Delta\mu$, the Monte Carlo data have been averaged over 77–150 runs, with error bars showing the standard error. A line of slope 1/4 has been shown to facilitate comparison with the power law $L(t) \sim t^{1/4}$. The characteristic time when we would expect a change in growth law on the basis of Eq. (12) and using $f_p(T = 2J_2, \theta = \pi/4) \approx 6.75J_2$ is $t_c \approx 3\times10^2$, $1\times10^4$, $2\times10^6$, and $8\times10^9$ for $\Delta\mu = 2.0$, 1.2, 0.8, and 0.5, respectively.

(12). For $|\Delta\mu|/J_2 = 1.2$ and 2.0, there is a regime where the effective power law approaches (although remains a bit less than) 1/4.

Also visible for $|\Delta\mu|/J_2 = 2.0$, and just barely for $|\Delta\mu|/J_2 = 1.2$, is a rather sharp leveling off in the growth of $L(t)$ at late times. Studying the configurations at these late times, we find that the system appears to have reached a steady state in which at any time, there are structures such as ledges because the crystal is in the process of growing (or shrinking), due to the nonzero value of $\Delta\mu$. The fact that such growth is in progress puts a maximum limit on the average facet size. [Our measure of $L(t)$ as being inversely proportional to the total length of boundary between the different facet orientations may also be underestimating somewhat the true value of the characteristic length scale. See Sec. IV C of Ref. [13].] A more detailed study of correlation functions might be useful in further characterizing this behavior (e.g., one might even find a breakdown of scaling). Clearly, these are effects that occur in a regime beyond which our assumption of being very near equilibrium is valid.

In closing this section, we briefly discuss the likely effects of a nonzero chemical potential difference in the temperature regime $T_{CR} < T < T_{ER}$. Here the coarsening is already expected to be a power law for $\Delta\mu = 0$. A nonzero $\Delta\mu$ seems unlikely to do more than alter the prefactor of the power law. One important question, however, is whether it might provide a relevant perturbation that will break the symmetry associated with the conical point and thus allow the selection of two particular orientations for the surface to separate into. In the absence of a renormalization group picture for the conical point on the ECS, we do not know how to determine if this perturbation is relevant and hence this question remains unanswered.

## V. SUMMARY AND CONCLUSIONS

In this paper, we have considered the phase separation of crystal surfaces within an Ising lattice gas model for materials with the sodium chloride structure. We found that, depending on the temperature and growth conditions, a number of interesting behaviors can be observed.

For a crystal in equilibrium with its vapor, we argued that the coarsening of the surface structure will be logarithmic in time for temperatures below the corner rounding transition temperature $T_{CR}$, where an arbitrary surface $[hkl]$ (with $h$, $k$, $l > 0$) undergoes three-phase separation into the smooth [100], [010], and [001] facets. Such sluggish dynamics occur because the coarsening process involves the creation of steps across the smooth facets and these steps have a nonzero free energy per unit length below $T_{CR}$. Since the discreteness of the system plays a fundamental role here, recently proposed continuum models for the dynamics of phase separation of surfaces fail to capture this effect.

At all temperatures between $T_{CR}$ and the edge-rounding temperature $T_{ER}$, some surface orientations remain unstable. It appears likely, based on the exact solution of a related model, that (because of a spontaneously generated symmetry) such surfaces will generically undergo decomposition into an entire one-parameter family of surfaces. This process, analogous to phase ordering in an $XY$ (or Heisenberg) model, should obey $L(t) \sim t^{1/4}$. Only if effects not considered (such as elastic interactions or surface melting) break the spontaneously generated symmetry does the possibility exist for simple two-phase separation. In that case, the growth law will be $L(t) \sim t^n$, with either $n = 1/3$ or $n = 1/4$.

Such an algebraic growth law should also hold at late enough times *below* $T_{CR}$ for the case of *driven* surfaces, i.e., where the crystal and vapor are not in equilibrium (crystal growth, or etching), with the crossover time from very slow (approximately logarithmic) to power-law growth diverging rapidly as the chemical potential difference between crystal and vapor decreases to zero. We noted the close analogy in this case to the growth of a crystal facet by nucleation below the roughening transition.

In closing, we should mention some effects that have been neglected in our microscopic model and could conceivably be important in real materials. First, there are impurities and defects that may act to speed up the phase separation of surfaces, just as they do for the growth of crystal surfaces below the roughening transition [38,56]. This could be particularly important given that impurities often tend to segregate to the surface, so that even reasonably pure samples can have fairly dirty surfaces. Second, there are also elastic effects, which have been discussed in recent work [14,15,57,58] as possibly slowing

down the faceting process and even stabilizing the system at a maximum facet size. There is some recent experimental evidence that seems to support this scenario [10]. Finally, there is the possibility of surface melting [40,49] and surface reconstructions [12], which can result in a more complicated ECS. Clearly these issues must all be addressed in order to obtain a realistic picture of the thermal faceting in real materials.

## ACKNOWLEDGMENTS

We would like to thank Alan Bray, Mark Holzer, Fong Liu, Michael Plischke, Jim Sethna, Martin Siegert, Henk van Beijeren, and Michael Wortis for helpful discussions. This work was supported by the NSERC of Canada.

## APPENDIX: CALCULATION OF THE STEP FREE ENERGY AND RELATED QUANTITIES

Here we calculate the step free energy $f_s(T,\theta)$ as a function of temperature $T$ and step angle $\theta$ (measured with respect to one of the lattice axes) within the [111] RSOS approximation. We then use this result to discuss features of the phase separation problem in the temperature regimes both below and above $T_{\rm CR}$. The reader is also referred to Ref. [20], where a calculation of the step free energy was performed from a somewhat different, but related, perspective.

It is in general quite difficult to compute the step free energy in a so-called canonical ensemble, where we restrict the step to have a certain angle. The easier route is to compute the step free energy in the grand canonical ensemble, where we do not constrain the step angle, but instead apply a field $\tilde{h}$ which couples to the angle of the step and thus allows us to control the average step angle [59]. To obtain $f_s(T,\theta)$ from $f_s(T,\tilde{h})$ we then need only determine this average step angle $\theta$ as a function of $\tilde{h}$. Then, $f_s(T,\theta)$ is related to $f_s(T,\tilde{h})$ by a Legendre transform, which has an intuitive physical interpretation.

In the [111] RSOS approximation, a step across, say, a [100] surface consists simply of a one-dimensional series of plaquettes of either the [010] or the [001] orientation [see, e.g., Fig. 4(b)]. If we apply a field $\tilde{h}$ in order to favor one orientation over another, then the Hamiltonian for the step is equivalent to that for a one-dimensional Ising model in a magnetic field. Within this grand canonical ensemble, there are several routes to calculate the step free energy. If one makes the analogy to the Ising model then one can write down the free energy *per plaquette* [20]. This is done most easily by using a transfer matrix [60]. However, to make connections to free energy barriers, we find it most natural to compute the free energy *per unit projected length along one of the lattice axes.*

The calculation proceeds as in Sec. II of Ref. [13], except with the addition of a field term $-m_i\tilde{h}$ to the energy of a column in Eq. (2.10) of [13]. Here we are interested only in the large-size ($L\to\infty$) limit in which we can write the partition function as

$$Z(L)=e^{-4J_2L/T}\left[1+\frac{e^{-(8J_2-\tilde{h})/T}}{1-e^{-(4J_2-\tilde{h})/T}}\right]^L , \tag{A1}$$

where $L$ is the projected length along the [010] axis. The quantity $f_p(T,\tilde{h})$, a free energy per unit projected length at a given applied field $\tilde{h}$ is then

$$\begin{aligned} f_p(T,\tilde{h}) &= -\frac{T}{L}\ln[Z(L)] \\ &= 4J_2 - T\ln\left(1+\frac{q^2H}{1-qH}\right) , \end{aligned} \tag{A2}$$

where $q\equiv\exp(-4J_2/T)$ and $H\equiv\exp(\tilde{h}/T)$. The (average) tangent of the angle of the step with respect to the [010] axis is given by

$$\begin{aligned} \tan(\theta) &= -\frac{\partial f_p(T,\tilde{h})}{\partial\tilde{h}} \\ &= \frac{q^2H}{(1-qH)(1-qH+q^2H)} . \end{aligned} \tag{A3}$$

This equation can be inverted in order to express $\tilde{h}$ as a function of $r\equiv\tan(\theta)$:

$$\tilde{h}=T\ln\left[\frac{(2-q)r+q-\sqrt{(r^2+1)q^2+2(2-q)qr}}{2q(1-q)r}\right] . \tag{A4}$$

The step free energy as a function of angle is then given by

$$f_s(T,\theta)=[f_p(T,\tilde{h})+\tilde{h}\tan(\theta)]\cos(\theta) , \tag{A5}$$

where, for a given angle $\theta$, $\tilde{h}$ is determined by (A4). The addition of $\tilde{h}\tan(\theta)$ takes the Legendre transform of $f_p(T,\tilde{h})$ to give us $f_p(T,\theta)$. The physical interpretation of this transform is simply that this term subtracts off, from $f_p(T,\tilde{h})$, the energy contribution due to the coupling of the field to the angle, thus leaving us with what the free energy of a step at angle $\theta$ would be in the absence of any applied field. The factor $\cos(\theta)$ is necessary to give us the free energy per unit (macroscopic) step length $f_s$ rather than the free energy per unit projected length $f_p$.

There are two ways in which the calculation above is useful to us. First, for $T<T_{\rm CR}$ and $\Delta\mu=0$, the free energy barrier per unit length for shrinking of a cubical projection of edge length $L$ (in the large $L$ limit) is given rigorously by $f_B(T)\equiv f_p(T,\tilde{h}=0)$. This is also, roughly speaking, the appropriate barrier to consider for a coarsening surface (as discussed in Sec. III A), although the value of $f_B(T)$ can no longer be so rigorously determined. In particular, it would depend on precisely how we choose to define the characteristic length scale $L$. For coarsening in the case $\Delta\mu\neq0$, the important quantity that enters into the equations is $f_p(T,\theta=\pi/4)$, as discussed in Sec. IV.

Second, we can extend the above results to derive the

opening angle $\theta_c(T)$, discussed in Sec. III B, in the temperature regime $T_{CR} < T < T_{ER}$. To determine this angle, we consider a surface $[hkl]$ with $0 \leq k \leq h$ and $0 \leq l \ll h$. Such a surface is thus very close to being a $[hk0]$ surface and if it is unstable then (independent of which of the conical point or ridge scenarios discussed in Sec. III B is correct), it will break up (at least primarily) into surfaces that are vicinal to the [100] orientation and surfaces that are vicinal to the [010] orientation. These surfaces will have steps across them of a definite angle, given by $\theta_c(T)$. This opening angle is then determined by the condition that it minimize the total free energy of the resulting surface subject to the constraint that the surface has the correct average tilt in the $\hat{z}$ direction. The free energy of the surface is given by $f_s(T,\theta)L_s$, where $L_s$ is the total length of step. The tilt is given by $L_s \sin(\theta)$. Therefore, $\theta_c(T)$ is that angle $\theta$ which minimizes the quantity $f_s(T,\theta)/\sin(\theta)$ [61]. This one-dimensional minimization can easily be performed numerically. The results are shown in Fig. 7.


[1] For reviews, see A. J. W. Moore, in *Metal Surfaces: Structure, Energetics, and Kinetics* (American Society for Metals, Metals Park, OH, 1963), p. 155; M. Flytzani-Stephanopoulos and L. D. Schmidt, Prog. Surf. Sci. **9**, 83 (1979).

[2] H.-J. Ernst, F. Fabre, R. Folkerts, and J. Lapujoulade, Phys. Rev. Lett. **72**, 112 (1994); M. D. Johnson *et al.*, *ibid.* **72**, 116 (1994).

[3] M. Siegert and M. Plischke, Phys. Rev. Lett. **73**, 1517 (1994), and private communication.

[4] J. S. Ozcomert, W. W. Pai, N. C. Bartelt, and J. E. Reutt-Robey, Phys. Rev. Lett. **72**, 258 (1994).

[5] H. Kahata and K. Yagi, Jpn. J. Appl. Phys. **28**, L858 (1989); A. V. Latyshev, A. L. Aseev, A. B. Krasilnikov, and S. I. Stenin, Surf. Sci. **213**, 157 (1989); M. J. Ramstad *et al.*, Europhys. Lett. **24**, 653 (1993).

[6] J. Krug and H. T. Dobbs, Phys. Rev. Lett. **73**, 1947 (1994).

[7] C. Herring, Phys. Rev. **82**, 87 (1951); in *Structure and Properties of Solid Surfaces*, edited by R. Gomer and C. S. Smith (University of Chicago Press, Chicago, 1953), p. 5; Surf. Sci. **2**, 320 (1964).

[8] D. Knoppik and A. Losch, J. Cryst. Growth **34**, 332 (1976); D. Knoppik and F.-P. Penningsfeld, *ibid.* **37**, 69 (1977).

[9] W. W. Mullins, J. Appl. Phys. **28**, 333 (1957); Acta Metall. **6**, 414 (1958); J. Appl. Phys. **30**, 77 (1959); Philos. Mag. **6**, 1313 (1961).

[10] R. J. Phaneuf, N. C. Bartelt, E. D. Williams, W. Swiech, and E. Bauer, Phys. Rev. Lett. **67**, 2986 (1991).

[11] R. J. Phaneuf, N. C. Bartelt, E. D. Williams, W. Swiech, and E. Bauer, Phys. Rev. Lett. **71**, 2284 (1993).

[12] G. M. Watson, D. Gibbs, D. M. Zehner, M. Yoon, and S. G. J. Mochrie, Phys. Rev. Lett. **71**, 3166 (1993); M. Yoon, S. G. J. Mochrie, D. M. Zehner, G. M. Watson, and D. Gibbs, Phys. Rev. B **49**, 16 702 (1994); S. Song, S. G. J. Mochrie, and G. B. Stephenson (unpublished); and referenes therein.

[13] J. D. Shore, M. Holzer, and J. P. Sethna, Phys. Rev. B **46**, 11 376 (1992); see also Ref. [55].

[14] J. Stewart and N. Goldenfeld, Phys. Rev. A **46**, 6505 (1992).

[15] F. Liu and H. Metiu, Phys. Rev. B **48**, 5808 (1993).

[16] D. G. Vlachos, L. D. Schmidt, and R. Aris, Phys. Rev. B **47**, 4896 (1993).

[17] J. C. Heyraud and J. J. Métois, J. Cryst. Growth **84**, 503 (1987).

[18] Another possibility that has been discussed [10,14,15,57,58] is that elastic stresses set an upper bound on the size of the coarsening facets.

[19] C. Rottman and M. Wortis, Phys. Rev. B **29**, 328 (1984); Phys. Rep. **103**, 59 (1984).

[20] A.-C. Shi and M. Wortis, Phys. Rev. B **37**, 7793 (1988).

[21] G. S. Grest and D. J. Srolovitz, Phys. Rev. B **32**, 3014 (1985).

[22] J. D. Shore and D. J. Bukman, Phys. Rev. Lett. **72**, 604 (1994); D. J. Bukman and J. D. Shore, J. Stat. Phys. **78**, 1277 (1995).

[23] P. Curie, Bull. Soc. Min. France **8**, 145 (1885); J. W. Gibbs, Trans. Conn. Acad. **3**, 343 (1878); G. Wulff, Z. Krist. **34**, 449 (1901).

[24] M. Wortis, in *Chemistry and Physics of Solid Surfaces VII*, edited by R. Vanselow and R. F. Howe (Springer-Verlag, Berlin, 1988), p. 367.

[25] H. van Beijeren, Phys. Rev. Lett. **38**, 993 (1977).

[26] C. Jayaprakash and W. F. Saam, Phys. Rev. B **30**, 3916 (1984).

[27] H. W. J. Blöte and H. J. Hilhorst, J. Phys. A **15**, L631 (1982); B. Nienhuis, H. J. Hilhorst, and H. W. J. Blöte, *ibid.* **17**, 3559 (1984).

[28] The [111] RSOS model for a cubic crystal *with interactions corresponding to the Hamiltonian specified by Eq. (1)* was first studied in [20]. However, the model itself had been introduced in two earlier papers (Ref. [27]). In the first of these, the crystal shape was studied for a cubic crystal with nearest-neighbor attractive interactions, while in the second, more complicated interactions were considered. However, in neither case did the interactions studied lead to missing orientations on the crystal shape, which will be our interest here.

[29] Technically speaking, one should be concerned that the electrostatic interaction between ions would be expected to be long ranged. However, this problem can be avoided by considering the elementary units to be cubes of eight atoms that again sit on a cubic lattice (with twice the atomic lattice spacing) and have only octopolar interactions between them. For details, see [20].

[30] Throughout this paper, we measure temperature in units of energy, i.e., we set $k_B \equiv 1$.

[31] We use the notation {100} to refer to the set of surface orientations that includes the [100] and all symmetrically equivalent orientations.

[32] It is tempting to claim that $T_{CR}$ being above room temperature explains the sharp cubical shapes seen in ordinary grains of table salt. However, such grains were formed by grinding and are not in equilibrium with their vapor. Thus, while one might make the general point that these grains show the basic preference of NaCl to expose its {100} facets, any attempt to make a more detailed correspondence between equilibrium shapes and

table salt should probably be "treated with a grain of salt."

[33] A. F. Andreev, Zh. Eksp. Teor. Fiz. **80**, 2042 (1981) [Sov. Phys. JETP **53**, 1063 (1981)].

[34] We use the same symbol $h$ both here and in expressing surface orientations as $[hkl]$, but trust that our meaning is always clear from context.

[35] V. L. Pokrovsky and A. L. Talapov, Phys. Rev. Lett. **42**, 65 (1979).

[36] D. G. Vlachos (private communication).

[37] S. T. Chui and J. D. Weeks, Phys. Rev. Lett. **40**, 733 (1978).

[38] J. D. Weeks and G. H. Gilmer, Adv. Chem. Phys. **40**, 157 (1979).

[39] P. Nozières, in *Solids Far From Equilibrium*, edited by C. Godrèche (Cambridge University Press, Cambridge, 1992), p. 1.

[40] H. van Beijeren and I. Nolden, in *Structure and Dynamics of Surfaces II*, edited by W. Schommers and P. Von Blackenhagen Topics in Current Physics Vol. 43 (Springer-Verlag, Berlin, 1987), p. 259.

[41] There may be some other possible scenarios too if one allows for the possibility that the boundary between the facets and the curved parts of the ECS could be first order (i.e., a sharp edge). This cannot be rigorously ruled out, although if step interactions are repulsive because of entropic considerations, one *usually* seems to find second-order transitions (of the Pokrovsky-Talapov type [35]) at the facet boundaries. [See C. Jayaprakash, C. Rottmann, and W. F. Saam, Phys. Rev. B **30**, 6549 (1984); T. Yamamoto and T. Izuyama, J. Phys. Soc. Jpn. **56**, 632 (1987); and Refs. [24,26]].

[42] In Ref. [22], we noted how the projected surface tension has the linear form $F(\psi_1, \psi_2) = A|\psi_1|$ in the coexistence regions if there is a conical point. Here $(\psi_1, \psi_2)$ are two independent variables specifying the surface orientation and chosen such that $\psi_1$ measures tilts of the ECS in the direction along the ridge between the facets. Within the ridge scenario, by contrast, the projected surface tension has the form $F(\psi_1, \psi_2) = Af(|\psi_1|)$ in the coexistence regions, where $f(|\psi_1|)$ is a function with positive first and second derivatives.

[43] The ridge scenario also corresponds more closely to the situation that occurs in the three-state Potts model in two dimensions when one considers the phase diagram as a function of applied fields at constant temperature $T$ in the range $T_C^{(3)} < T < T_C^{(2)}$. Here $T_C^{(3)}$ is the critical temperature of the three-state Potts model and $T_C^{(2)}$ is the critical temperature for the two-state Potts (i.e., the Ising) model. However, in that case, there is nothing equivalent to the facets and one has three first-order lines coming in from infinite fields along three different directions, with each line terminating in a second-order critical point. [See J. P. Straley and M. E. Fisher, J. Phys. A **6**, 1310 (1973). For related reviews, see I. D. Lawrie and S. Sarbach, in *Phase Transitions and Critical Phenomena*, edited by C. Domb and J. L. Lebowitz (Academic, London, 1984), Vol. 9; F. Y. Wu, Rev. Mod. Phys. **54**, 235 (1982).]

[44] This fcc model, however, is likely less physically relevant since the interactions do not have a simple interpretation in terms of real materials: Because some of the nearest neighbors of the nearest neighbors of a lattice site $A$ are themselves nearest neighbors of site $A$, there is no way to decorate the sites of an fcc lattice with atoms in such a way that the nearest neighbors of a given atom are all of unlike species while the next nearest neighbors are all of like species.

[45] E. H. Lieb, Phys. Rev. Lett. **18**, 692 (1967); C. P. Yang, *ibid.* **19**, 586 (1967); B. Sutherland, C. N. Yang, and C. P. Yang, *ibid.* **19**, 588 (1967); see also C. N. Yang and C. P. Yang, Phys. Rev. **150**, 321 (1966); **150**, 327 (1966).

[46] For a review, see E. H. Lieb and F. Y. Wu, in *Phase Transitions and Critical Phenomena*, edited by C. Domb and M. S. Green (Academic, London, 1972), Vol. 1; also see I. Nolden, J. Stat. Phys. **67**, 155 (1992); Ph.D. thesis, University of Utrecht, 1990.

[47] Curiously enough, the original explanation of the solution to the six-vertex model by Sutherland, Yang, and Yang [45] has an incorrect phase diagram that corresponds to neither the ridge nor the conical point scenarios. Instead, their phase diagram corresponds to having all surface orientations stable at any nonzero temperature, except perhaps for those marginal orientations parallel to the edge.

[48] J. Neergaard and M. den Nijs, Phys. Rev. Lett. **74**, 730 (1995).

[49] H. van Beijeren (private communication).

[50] J. S. Langer, in *Solids Far From Equilibrium* (Ref. [39]), p. 297.

[51] A. J. Bray, in *Phase Transitions in Systems with Competing Energy Scales*, Vol. X of *NATO Advanced Study Institute, Series C: Mathematical and Physical Sciences,* edited by T. Riste and D. Sherrington (Kluwer Academic, Dordrecht, 1993), p. 405; Phys. Rev. Lett. **62**, 2841 (1989); A. J. Bray and A. D. Rutenberg, Phys. Rev. E **49**, R27 (1994).

[52] D. A. Huse, Phys. Rev. B **34**, 7845 (1986); J. G. Amar, F. E. Sullivan, and R. D. Mountain, *ibid.* **37**, 196 (1988); C. Roland and M. Grant, *ibid.* **39**, 11 971 (1989).

[53] J. D. Shore (unpublished).

[54] M. Mondello and N. Goldenfeld, Phys. Rev. E **47**, 2384 (1993).

[55] J. D. Shore, Ph.D. thesis, Cornell University, 1992.

[56] G. H. Gilmer, Science **208**, 355 (1980).

[57] O. L. Alerhand, D. Vanderbilt, R. D. Meade, and J. D. Joanopoulos, Phys. Rev. Lett. **61**, 1973 (1988); O.L. Alerhand *et al.*, *ibid.* **64**, 2406 (1990).

[58] V. I. Marchenko, Zh. Eksp. Teor. Fiz. **81**, 1141 (1981) [Sov. Phys. JETP **54**, 605 (1981)].

[59] M. Holzer, Ph.D. thesis, Simon Fraser University, 1990.

[60] K. Huang, *Statistical Mechanics*, 2nd ed. (Wiley, New York, 1987), pp. 361–363.

[61] Note that $\theta_c(T)$ is *not* determined simply by the condition $f_s(T, \theta) = 0$, as one would find if one simply compared the surface's free energy to that of a surface that decomposes into the [100], [010], and [001] surface orientations. This is because even a surface that cannot lower its free energy by decomposing into these facet orientations may still be able to lower its free energy by breaking up into other surface orientations.

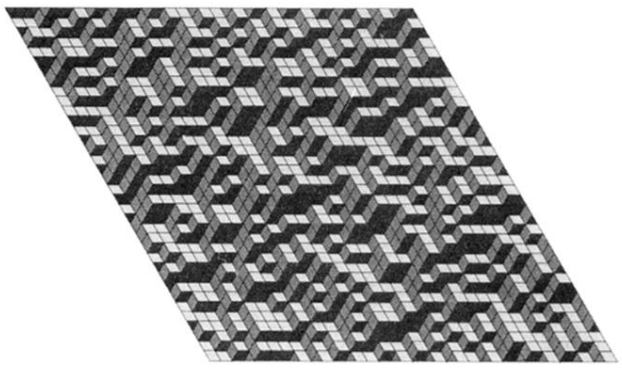

(a)

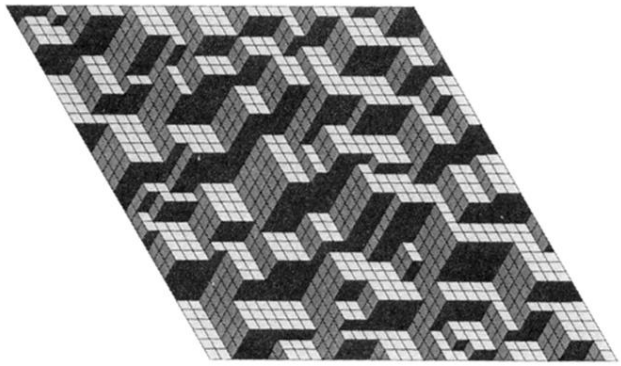

(b)

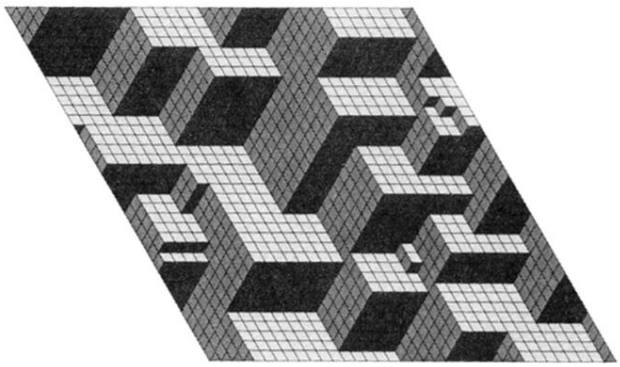

(c)

FIG. 1. Decomposition of a surface in the [111] RSOS model for the Hamiltonian of Eq. (1) at $T < T_{\mathrm{CR}}$. Shown is a [111] surface that has been quenched from infinite temperature to $T = 3J_2$ at times (a) $t = 0$, (b) $t = 100$, and (c) $t = 10\,000$ (in MC steps per plaquette) following the quench.

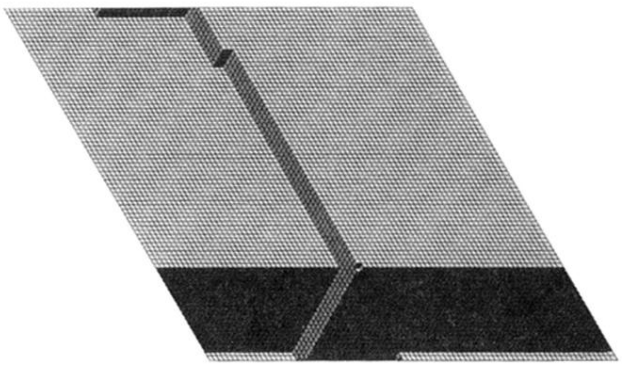

(a)

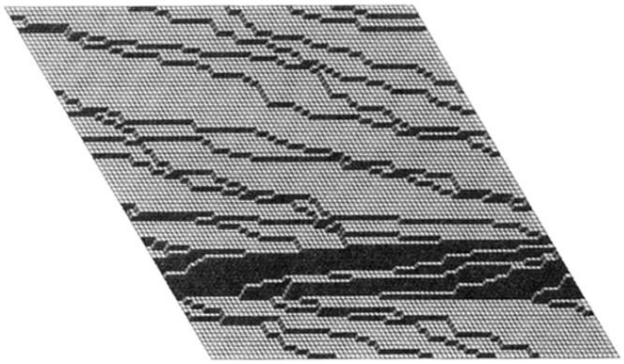

(b)

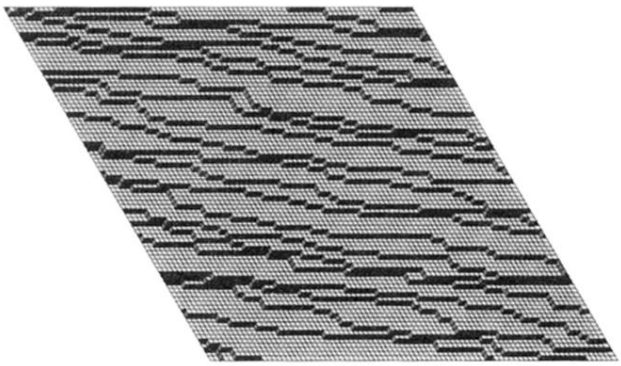

(c)

FIG. 4. Equilibrium configurations for a [15,5,1] surface in the [111] RSOS model at various temperatures: (a) $T = 4J_2$, (b) $T = 14J_2$, and (c) $T = 34J_2$. Minimization of the total surface free energy, under the assumption that the surface is close enough to being vicinal that the steps do not interact, gives $T_{\mathrm{PS}}([15,5,1]) \approx 22.6J_2$ for the phase separation temperature (see the Appendix and Fig. 7). This estimate should provide an upper bound for the actual value of $T_{\mathrm{PS}}([15,5,1])$.

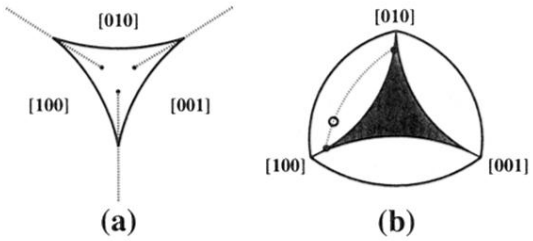


FIG. 5. The "ridge scenario." In (a) we show a closeup of the corner region of the ECS for $T_{\rm CR} < T < T_{\rm ER}$, under the assumption that the sharp edges between the facets continue into the curved part of the ECS, finally terminating at second-order critical points. At any point along this edge, there is "coexistence" between two surface orientations. (Here sharp first-order edges are shown by dashed lines while the second-order Pokrovsky-Talapov boundaries between the facets and the curved part of the ECS are shown by solid lines. The solid circles represent second-order critical points at the end of the first-order lines.) In (b) we present the diagram of the stable surface orientations, showing how any unstable surface will phase separate into the two coexisting stable surfaces. In our example, any orientation along the dashed curve (such as the one indicated by the open circle) decomposes into the two (marginally) stable surface orientations indicated by the solid circles.

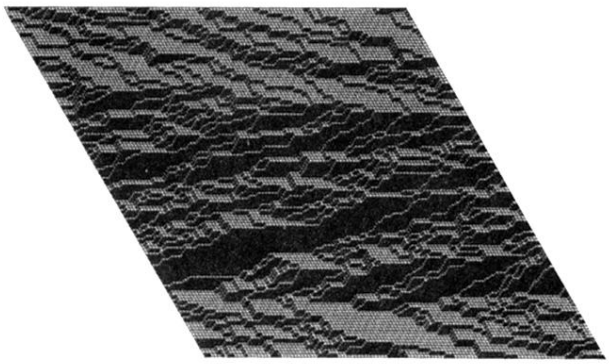

FIG. 8. Equilibrium configuration for a [13,13,4] surface in the [111] RSOS model at $T = 8J_2$. Note that the surface appears to have phase separated, but the equilibrium state is quite complicated. This may be an indication that many different surface orientations are involved, as one would expect from the conical point scenario.

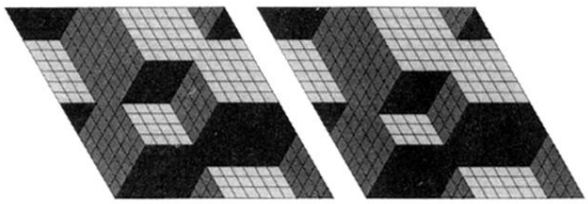

(a) (b)

FIG. 9. Shrinking a cubical projection in the [111] RSOS model. (a) Cubical projection with $L = 4$. (b) Same projection once one face has been removed. For $\Delta\mu \geq 0$, this configuration is lower in energy than that of (a) by $4J_2 + \Delta\mu L^2$.